



Missouri University of Science and Technology
Scholars' Mine

Electrical and Computer Engineering Faculty
Research & Creative Works

Electrical and Computer Engineering

01 Jan 2003

Multilevel Converter-Based Dual-Frequency Induction Heating Power Supply

B. Diong

S. Basireddy

Keith Corzine

Missouri University of Science and Technology

Follow this and additional works at: https://scholarsmine.mst.edu/ele_comeng_facwork

 Part of the [Electrical and Computer Engineering Commons](#)

Recommended Citation

B. Diong et al., "Multilevel Converter-Based Dual-Frequency Induction Heating Power Supply," *Proceedings of the 29th Annual Conference of the IEEE Industrial Electronics Society, IECON '03. (2003, Roanoke, VA)*, Institute of Electrical and Electronics Engineers (IEEE), Jan 2003.

The definitive version is available at <https://doi.org/10.1109/IECON.2003.1280366>

This Article - Conference proceedings is brought to you for free and open access by Scholars' Mine. It has been accepted for inclusion in Electrical and Computer Engineering Faculty Research & Creative Works by an authorized administrator of Scholars' Mine. This work is protected by U. S. Copyright Law. Unauthorized use including reproduction for redistribution requires the permission of the copyright holder. For more information, please contact scholarsmine@mst.edu.

Multilevel Converter-based Dual-frequency Induction Heating Power Supply

Bill Diong and Sarala Basireddy

Department of Electrical and Computer Engineering
The University of Texas at El Paso
El Paso, TX 79968, USA
bdiong@ece.utep.edu

Keith Corzine

Department of Electrical Engineering and Computer Science
University of Wisconsin – Milwaukee
Milwaukee, WI 53201, USA
keith@corzine.net

Abstract – Most existing power supplies for induction heating equipment produce voltage at a single (adjustable) frequency. Recently, however, induction heating power supplies that produce voltage at two (adjustable) frequencies have been researched and even commercialized. Dual-frequency power supplies are a significant development for heat-treating workpieces with uneven geometries, such as gears, since different portions of such workpieces are heated dissimilarly at a single frequency and so require a two step process using a single-frequency power supply. On the other hand, a dual-frequency power supply can achieve the desired result for such workpieces in a one step process. However, the existing approaches to dual-frequency voltage generation could be improved to achieve higher efficiency, improved control, reduced electromagnetic interference and greater reliability. This paper proposes the use of multilevel converters for providing induction heating power at two frequencies simultaneously. It also describes how the stepping angles for the desired output from this converter were determined. Furthermore, experimental results are presented as a verification of the analysis.

I. INTRODUCTION

Present-day manufacturing facilities require the precise, deliberate application of heat to targeted workpiece sections as part of numerous processes. These processes include hardening, brazing, annealing, tempering, bonding or removal, and pre-heating or melting. One important approach to workpiece heating is by electromagnetic induction and this is referred to as induction heating. For electromagnetic induction to occur, the workpiece and an induction coil (conductor) need to be in close proximity to each other (but not in contact). Then as an alternating current flows through the induction coil, the resulting electromagnetic field passes through and induces an equal and opposing electric current in the nearby workpiece, with the workpiece then heating up due to resistance to the induced current flow. The depth of penetration and the rate of heating of the workpiece depends on the induced current's frequency, the induced current's intensity, the specific heat of the material, the material's magnetic permeability, and the resistance to the flow of current. Consequently, the frequency and power level of the current passing through the induction coil are crucial variables for obtaining the optimal result.

Most commercially available power supplies for induction heating equipment rely on the use of resonant

circuits (hence they're referred to as resonant power converters [1–2]) to produce voltage at some single (adjustable) frequency. Recently, however, induction heating power supplies that produce voltage at two selected frequencies simultaneously have been investigated [3–6] as well as commercially introduced [7]. This is because for workpieces with uneven geometries, such as gears, different portions of the workpiece requiring treatment are heated to dissimilar depths at a single frequency and so it needs to be processed in two steps using a single frequency power supply. Hence, it becomes desirable to have simultaneous dual-frequency power supplied to the coil for inductive heating to attain uniform treatment depth for such workpieces during just one pass of the process. Drawbacks of the approach proposed by [3] include the restriction of dual-frequency production to just the 1st and 3rd harmonics and the inability to independently adjust their levels and those of the adjacent (5th, 7th, etc.) harmonics, although some incremental improvements have recently been made to this approach [4–6]. Drawbacks of existing simultaneous dual-frequency products [6] include the significant power losses experienced by the high-frequency part of those units, since the devices involved have to switch at those high frequencies and the two disparate control methods for the low-frequency and high-frequency circuits. Circumventing the above-mentioned drawbacks while preserving the property of precise dual frequency and power level generation (with suppression of adjacent harmonics) would result in an improved induction heating power supply. This paper describes initial studies of a potentially improved dual-frequency induction heating power supply, based on multilevel converters, which may achieve higher efficiency, greater frequency and power level control, reduced electromagnetic interference and greater reliability.

Multilevel converters are a recent exciting development in the area of high-power systems. Several topologies exist, including the diode-clamped (neutral-point clamped), capacitor-clamped (flying capacitor), and cascaded H-bridge (shown in Fig. 1), etc., topologies. Presently, the typical operation of such converters is to produce approximately a single-frequency output voltage (illustrated in Fig. 2), though this could be either fixed (utility) or varying (motor drive) [8]. While [9] has introduced the concept of multilevel converters for multi-frequency induction heating, few analytical details were provided.

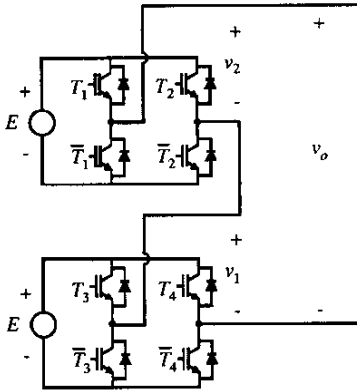


Fig. 1. Cascaded H-bridge (2-cell) multilevel converter circuit

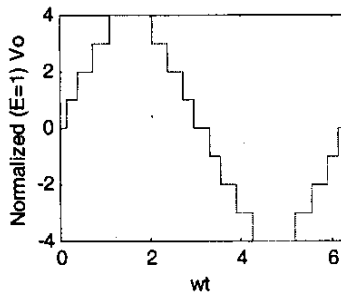


Fig. 2. 4-step, 9-level waveform

II. ANALYSIS

For an output voltage waveform that is quarter-wave symmetric (as in Fig. 2) with s positive steps of equal magnitude E , it is well-known that the waveform's Fourier series expansion is given by

$$v_o(t) = \sum_{\text{odd } h} \{ V_h \sin(h\omega t) \} \quad (1)$$

where

$$V_h = \frac{4E}{h\pi} [\cos(h\theta_1) + \cos(h\theta_2) + \dots + \cos(h\theta_s)] \quad (2)$$

and the θ_i , $i = 1, \dots, s$, are the angles (within the first quarter of each waveform cycle) at which the s steps occur. On the other hand, if a negative step (down) instead of a positive step (up) occurs at a particular θ_i , the coefficient of the corresponding cosine term in (2) is -1 instead of $+1$.

For the specific (introductory) problem of synthesizing a stepped waveform that has desired levels of V_1 and V_3 with two of the adjacent higher harmonics equal to zero, the stepping angles $0 \leq \theta_1 < \theta_2 < \dots < \theta_s \leq \pi/2$ must be chosen so that

$$\frac{4E}{\pi} [\cos(\theta_1) + \cos(\theta_2) + \dots + \cos(\theta_s)] = V_1 \quad (3a)$$

$$\frac{4E}{3\pi} [\cos(3\theta_1) + \cos(3\theta_2) + \dots + \cos(3\theta_s)] = V_3 \quad (b)$$

$$\cos(5\theta_1) + \cos(5\theta_2) + \dots + \cos(5\theta_s) = 0 \quad (c)$$

$$\cos(7\theta_1) + \cos(7\theta_2) + \dots + \cos(7\theta_s) = 0 \quad (d)$$

Again, for a waveform with a step down instead of a step up at a particular θ_i , the coefficient of the corresponding cosine term in (3) should be -1 instead of $+1$. Using the identities (also advocated by [10])

$$\cos(3\theta) = 4 \cos(\theta)^3 - 3 \cos(\theta) \quad (4a)$$

$$\cos(5\theta) = 16 \cos(\theta)^5 - 20 \cos(\theta)^3 + 5 \cos(\theta) \quad (b)$$

$$\cos(7\theta) = 64 \cos(\theta)^7 - 112 \cos(\theta)^5 + 56 \cos(\theta)^3 - 7 \cos(\theta) \quad (c)$$

and defining c_i as $\cos(\theta_i)$, (3) can be re-written as

$$\sum_{i=1, \dots, s} c_i = V_1 / \frac{4E}{\pi} = m_1 \quad (5a)$$

$$\sum_{i=1, \dots, s} \{ 4 c_i^3 - 3 c_i \} = V_3 / \frac{4E}{3\pi} = m_3 \quad (b)$$

$$\sum_{i=1, \dots, s} \{ 16 c_i^5 - 20 c_i^3 + 5 c_i \} = 0 \quad (c)$$

$$\sum_{i=1, \dots, s} \{ 64 c_i^7 - 112 c_i^5 + 56 c_i^3 - 7 c_i \} = 0 \quad (d)$$

Then the set of trigonometric equations (3) has been transformed into a set of multivariate polynomial equations (5), the solution of which is discussed in [11], for example.

Clearly, a necessary condition for the existence of nontrivial solutions to (5) is that the number of steps s be equal to or greater than the number of constraint equations. Consider now the two simplest problems of dual-frequency output voltage approximation by multilevel inverters:

- 2-step ($s = 2$) waveform with desired levels of 1st and 3rd harmonics, and
- 3-step ($s = 3$) waveform with desired levels of 1st and 3rd harmonics and simultaneous elimination of 5th harmonic.

A. 2-step waveform problem

There are two alternatives to consider: the PP case and PN case representing waveforms having two successive positive steps and a positive step followed by a negative step, respectively (see Fig. 3). Their negations, the NN case and NP case, simply result in solutions that are 180° phase-shifted respectively from the PP and PN solutions.

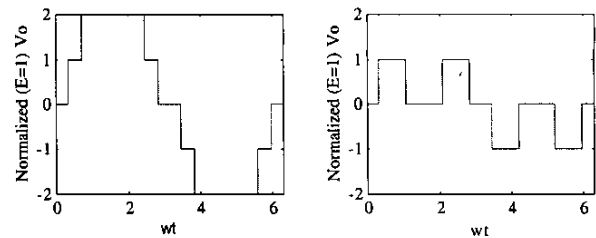


Fig. 3. 2-step waveform alternatives (PP and PN)

(i) PP case

The applicable equations are, from (5a) and (5b),

$$c_1 + c_2 = m_1 \quad (6a)$$

$$(4 c_1^3 - 3 c_1) + (4 c_2^3 - 3 c_2) = m_3 \quad (b)$$

Solving for c_1 and c_2 yields

$$c_1 = [3m_1^2 + \sqrt{3(3m_1^2 - m_1^4 + m_1 m_3)}] / 6 m_1 \quad (7a)$$

$$c_2 = [3m_1^2 - \sqrt{3(3m_1^2 - m_1^4 + m_1 m_3)}] / 6 m_1 \quad (b)$$

From (6a), note that for admissible c_1 and c_2 , m_1 is restricted to between 0 and 2. Moreover, since c_1 and c_2 need to be real and greater than 0, these constrain m_3 so that

$$m_1^3 - 3m_1 \leq m_3 \leq 4m_1^3 - 3m_1, \text{ for } 0 \leq m_1 \leq 1 \quad (8a)$$

$$m_1^3 - 3m_1 \leq m_3 \leq 4m_1^3 - 12m_1^2 + 9m_1, \text{ for } 1 \leq m_1 \leq 2 \quad (b)$$

The plot of these constraint curves in Fig. 4 for m_3 versus m_1 indicates (and confirmed analytically) that the range of possible m_3 is maximized at $m_1 = 1$. Then for $m_1 = 1$, the solutions for θ_1 and θ_2 are (they are unique) as shown in Fig. 5 as m_3 varies and the corresponding ratios of V_5 , V_7 and V_9 to V_1 are as shown in Fig. 6. Note that $V_3/V_1 = m_3/(3m_1)$.

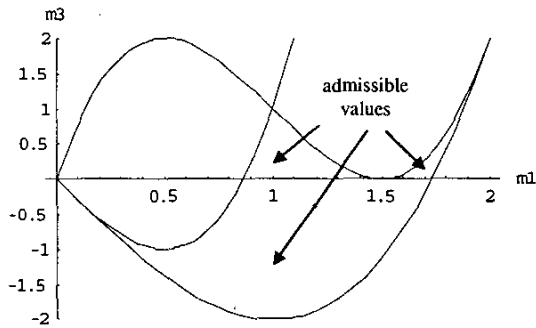


Fig. 4. Constraint curves for m_3 versus m_1 (PP case)

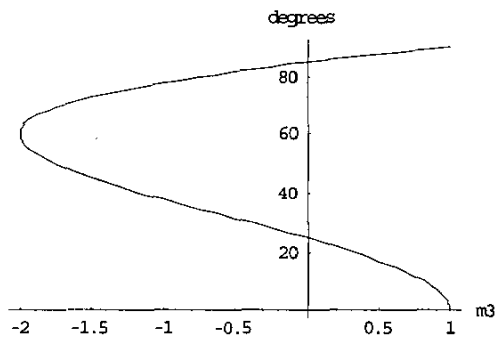


Fig. 5. Step angle solutions for θ_1 (lower) and θ_2 (upper) when $m_1 = 1$

The solutions for θ_1 and θ_2 as well as the associated higher harmonic amplitudes were also obtained at other allowable values of m_1 and m_3 , but these are not shown here due to space constraints. Note also that this case requires the production of a 5-level waveform and (at least) a 2-cell converter. With a 2-cell converter, it is possible to turn on and turn off each switch at the fundamental frequency to produce the desired waveform.

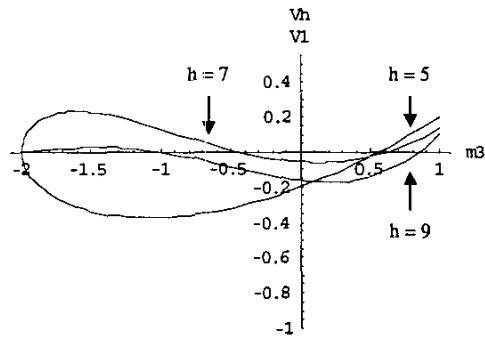


Fig. 6. Ratios of V_5 , V_7 and V_9 to V_1 for $m_1 = 1$

(ii) PN case

The applicable equations are

$$c_1 - c_2 = m_1 \quad (9a)$$

$$(4c_1^3 - 3c_1) - (4c_2^3 - 3c_2) = m_3 \quad (b)$$

where the second equation is obtained instead of (6b) because the second step is down instead of up. Then substituting (9a) into (9b) and solving for c_1 and c_2 yields

$$c_1 = [3m_1^2 + \sqrt{3(3m_1^2 - m_1^4 + m_1 m_3)}] / 6 m_1 \quad (10a)$$

$$c_2 = [-3m_1^2 + \sqrt{3(3m_1^2 - m_1^4 + m_1 m_3)}] / 6 m_1 \quad (b)$$

From (9a), note that for admissible c_1 and c_2 , m_1 is restricted to a value between 0 and 1. Moreover, since c_1 needs to be real and less than 1, this constrains m_3 such that

$$m_1^3 - 3m_1 \leq m_3 \leq 4m_1^3 - 12m_1^2 + 9m_1 \quad (11a)$$

whereas since c_2 needs to be real and greater than 0, this constrains m_3 such that

$$m_1^3 - 3m_1 \leq 4m_1^3 - 3m_1 \leq m_3 \quad (b)$$

The plot of the constraint curves in Fig. 7 for m_3 versus m_1 indicates (and confirmed analytically) that the range of possible m_3 yielding admissible solutions is maximized at $m_1 = 0.5$.

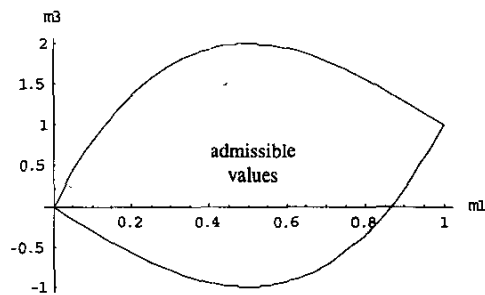


Fig. 7. Constraint curves for m_3 versus m_1 (PN case)

Then for $m_1 = 0.5$, the step angle solutions for θ_1 and θ_2 (they are unique) are as shown in Fig. 8 as m_3 varies and the ratios of V_5 , V_7 and V_9 to V_1 are as shown in Fig. 9.

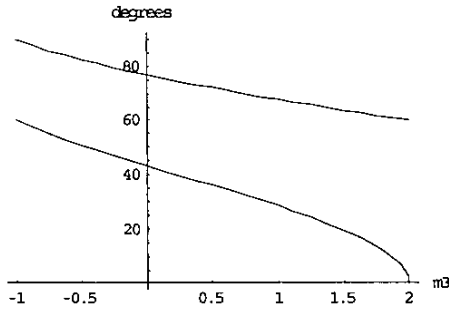


Fig. 8. Step angle solutions for θ_1 (lower) and θ_2 (upper) for $m_1 = 0.5$

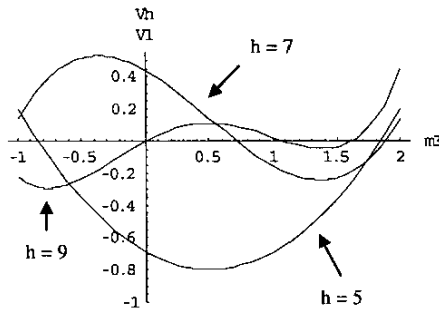


Fig. 9. Ratios of V_5 , V_7 and V_9 to V_1 for $m_1 = 0.5$

The solutions for θ_1 and θ_2 as well as the associated higher harmonic amplitudes were also obtained at other allowable values of m_1 and m_3 , but these are not shown here.

Note that this case requires the production of a 3-level waveform and (at least) a 1-cell converter. With a 1-cell converter, the switches can be operated so that each turns on and off at twice the fundamental frequency. With a 2-cell converter, it is possible to turn each switch on and off at the fundamental frequency to produce the desired waveform.

B. 3-step waveform problem

There are four, i.e., $\frac{1}{2}(2^3)$, possible combinations of 3-step waveforms to consider, excluding those that are the negations of the following cases: PPP, PPN, PNP and PNN.

The applicable equations are, from (5a), (5b) and (5c),

$$c_1 + k_2 c_2 + k_3 c_3 = m_1 \quad (12a)$$

$$(4c_1^3 - 3c_1) + k_2(4c_2^3 - 3c_2) + k_3(4c_3^3 - 3c_3) = m_3 \quad (b)$$

$(16c_1^5 - 20c_1^3 + 5c_1) + k_2(16c_2^5 - 20c_2^3 + 5c_2) + k_3(16c_3^5 - 20c_3^3 + 5c_3) = 0 \quad (c)$ where k_2, k_3 are separately either +1 or -1 for a positive step or a negative step, respectively. Substituting for c_3 from (12a) into (12b), (12c) then yields two (nonlinear) polynomial equations in terms of c_1 and c_2 . The exact solution of such equations (as opposed to running a search algorithm) is, in general, computationally intensive and increasingly difficult as the number of variables increases [11]. For two equations with two variables, however, the procedure is relatively straight forward as summarized in the Appendix.

In each case, we first determined the limits of m_1 and m_3 for the existence of admissible solutions from (12). These limits are defined by the requirement for c_1, c_2, c_3 to be real and, by definition of their relationship, for c_1 to be less than 1 and c_3 to be greater than 0. Then, as example, the value of m_1

yielding the maximum range of m_3 was determined and the step-angles for this m_1 value found by solving (12) iteratively for incrementally increasing values of m_3 . These solutions then allowed the higher harmonic amplitudes to be plotted.

(i) PPP case

Solutions exist and are probably unique (no multiple solutions have been found for the values of m_1 and m_3 tested so far) for the range of m_1 and m_3 delineated by the constraint curves of Fig. 10. The value of m_1 yielding the maximum range of m_3 is about 1.8. Plots of the step-angle solutions at this optimum and of the corresponding higher harmonic amplitudes are omitted due to length constraints. Note that this case requires the production of a 7-level waveform and (at least) a 3-cell converter. With a 3-cell converter, it is possible to turn on and turn off each switch at the fundamental frequency to produce the desired waveform.

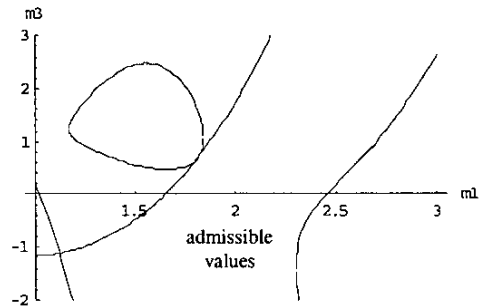


Fig. 10. Constraint curves for m_3 versus m_1 (PPP case)

(ii) PPN case

Solutions exist and are probably unique (no multiple solutions have been found for the values of m_1 and m_3 tested so far) for the range of m_1 and m_3 delineated by the constraint curves of Fig. 11. The value of m_1 yielding the maximum range of m_3 is about 1.1. Plots of the step-angle solutions at this optimum and of the corresponding higher harmonic amplitudes are omitted due to length constraints. Note that this case requires the production of a 5-level waveform and (at least) a 2-cell converter. But with a 3-cell converter, it is possible to turn on and turn off each switch at the fundamental frequency to produce the desired waveform, which is not possible with a 2-cell converter.

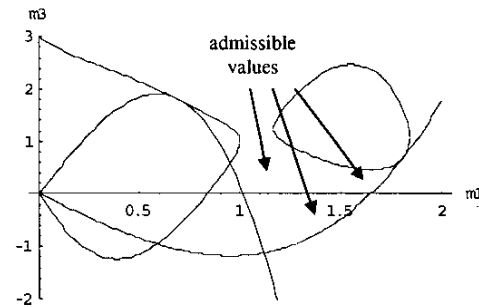


Fig. 11. Constraint curves for m_3 versus m_1 (PPN case)

(iii) PNP case

Solutions exist and are probably unique (no multiple solutions have been found for the values of m_1 and m_3 tested so far) for the range of m_1 and m_3 delineated by the constraint curves of Fig. 12. The value of m_1 yielding the maximum range of m_3 is about 0.588. Plots of the step-angle solutions at this optimum and of the corresponding higher harmonic amplitudes are shown in Fig. 13 and Fig. 14, respectively. Note that this case requires the production of just a 3-level waveform and (at least) a 1-cell converter. But with a 3-cell converter, it is possible to turn on and turn off each switch at the fundamental frequency to produce the desired waveform, which is impossible with a 1- or 2-cell converter.

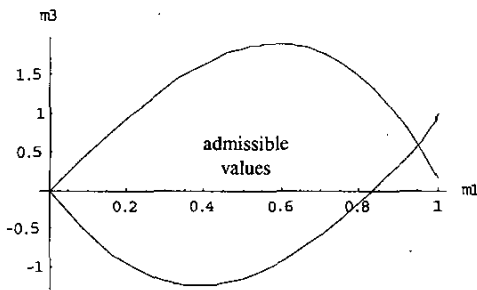


Fig. 12. Constraint curves for m_3 versus m_1 (PNP case)

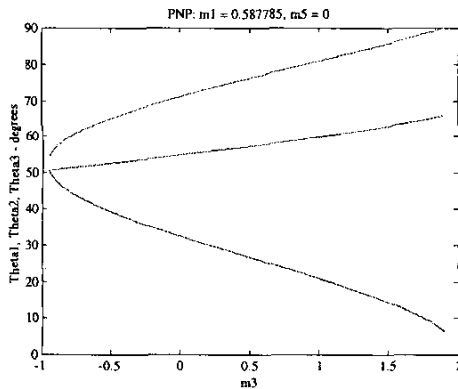


Fig. 13. Step angle solutions for PNP case maximum m_3 range

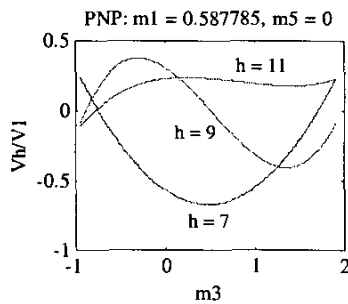


Fig. 14. Ratios of V_7 , V_9 and V_{11} to V_1

(iv) PNN case

Solutions exist and are probably unique (no multiple solutions have been found for the values of m_1 and m_3 tested so far) for the range of m_1 and m_3 delineated by the constraint curves of Fig. 15. The value of m_1 yielding the maximum range of m_3 is at 0, which is not useful. Plots of the step-angle solutions at this optimum and of the corresponding higher harmonic amplitudes are omitted due to the length constraint on this paper.

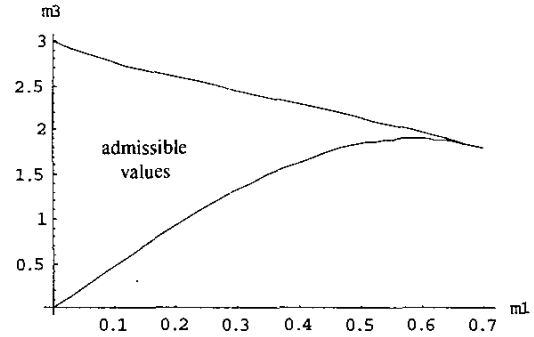


Fig. 15. Constraint curves for m_3 versus m_1 (PNN case)

Note that this case requires the production of just a 3-level waveform and (at least) a 1-cell converter. But with a 3-cell converter, it is possible to turn on and turn off each switch at the fundamental frequency to produce the desired waveform, which is impossible with a 1- or 2-cell converter.

C. 4-step waveform problem

The above investigation was extended in a similar manner to the 4-step/4-equation problem (corresponding exactly to (3) with $s = 4$) with desired levels of 1st and 3rd harmonics and simultaneous elimination of the 5th and 7th harmonics, and then to the more practical problem of producing 1st and 5th harmonics with simultaneous elimination of the 3rd and 7th harmonics, which however cannot be detailed here due to space constraints. However, the experimental result we present next is an example solution to the latter problem.

III. EXPERIMENTAL RESULTS

Laboratory measurements were obtained from a 5-level inverter demonstrating the 4-step PNPP case to generate desired 1st and 5th harmonic levels with $V_5/V_1 = 0.6$ while eliminating the 3rd and 7th harmonics. This waveform may be desired in an induction heating application where a span of 5 is needed between the two heating frequencies. Fig. 16 shows the voltage and current waveforms for a fundamental frequency of 10kHz. For this test, each DC voltage source (for a 2-cell cascaded H-bridge converter) was 125V, the (R-L) load average power was 513W and the conversion efficiency was 91.3% (with each switch operating at 20kHz). The step angles were set at $\theta_1 = 4.61^\circ$, $\theta_2 = 42.89^\circ$, $\theta_3 = 58.44^\circ$, $\theta_4 = 77.73^\circ$. Table 1 shows a comparison of the

analytical and measured harmonic amplitudes indicating good agreement between them. Note that the higher harmonics are mostly filtered out by the load inductance resulting mainly in the desired dual-frequency current.

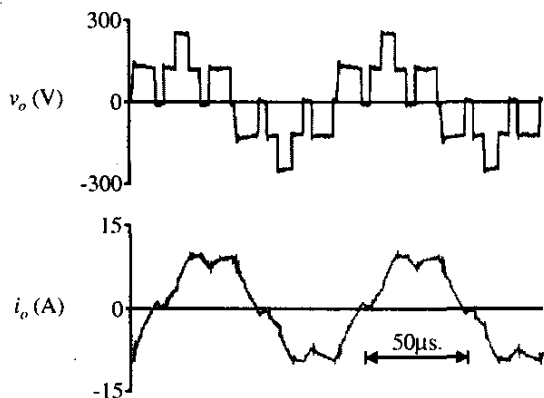


Fig. 16. 4-step, 5-level inverter measurements.

Table 1. 4-step 5-level inverter voltage harmonics.

	V_1	V_3	V_5	V_7	V_9	V_{11}	V_{13}	V_{15}
Analytical	159.1	0	95.5	0	3.2	7.5	31.4	7.6
Measured	156.8	2.7	98.1	2.2	3.0	10.1	33.9	7.6

IV. CONCLUSIONS

Only sporadic, off-line frequency and power level adjustments are needed for the induction heating application. So the step angles of a dual-frequency multilevel converter can be programmed as lookup tables depending on the desired components' frequency ratio and amplitude ratio.

For the 2-step case to generate desired levels of 1st and 3rd harmonics, the PP waveform results in lower harmonic distortion compared to the PN waveform but requires a 5-level waveform instead of a 3-level waveform. Moreover, for required magnitudes of $m_3 \leq 1$ with the PP waveform, positive m_3 is preferable to negative m_3 for reduced distortion. However, the PN waveform allows a broader range of achievable 1st and 3rd harmonic level combinations.

For the 3-step case, the PNP waveform allows for a broad range of achievable 1st and 3rd harmonic level combinations although yielding a fair amount of harmonic distortion. Moreover, it only requires producing a 3-level waveform. However, to have all devices operate at the fundamental frequency to produce this waveform still requires a 3-cell converter.

Finally, experimental results have been presented for the 4-step case that validates the proposed approach to dual-frequency voltage generation by multilevel converters.

V. REFERENCES

[1] M. K. Kazimierczuk and D. Czarkowski, *Resonant power converters*, John Wiley & Sons, Inc., New York, 1995.

[2] S. Kanchubotla and B. Diong, "A comparative guide to the main steady-state characteristics of four-element current-source resonant converters," *Proc. IECEC*, Washington, DC, Jul 2002.

[3] K. Matsuse, K. Nomura and S. Okudaira, "New quasi-resonant inverter for induction heating," *Power Conversion Conference, 1993. Yokohama 1993. Conference Record of the*, pp 117-122.

[4] K. Matsuse and S. Okudaira, "Power control of an adjustable frequency quasi-resonant inverter for dual frequency induction heating," *Proc. PIEMC*, volume: 2, pp 968-973, 2000.

[5] S. Okudaira and K. Matsuse, "Dual frequency output quasi-resonant inverter for induction heating," *Trans. Institute of Electrical Engineers of Japan*, vol. 121-D, no. 5, May 2001, pp 563-568.

[6] K. Matsuse and S. Okudaira, "A new quasi-resonant inverter with two-way short-circuit switch across a resonant capacitor," *Proc. Power Conversion Conf., 2002. PCC Osaka 2002*, volume: 3, pp 1496-1501.

[7] <http://www.eldec.de/engl/download/SDF-method.pdf>; *Simultaneous Dual Frequency Induction Heat Treating*.

[8] J. Rodriguez, J-S. Lai and F. Z. Peng, "Multilevel inverters: a survey of topologies, controls, and applications," *IEEE Trans. Industrial Electronics*, volume: 49, Aug 2002, pp 724-738.

[9] J. I. Rodriguez and S. B. Leeb, "A multilevel inverter topology for inductively-coupled power transfer," *Applied Power Electronics Conf., 2003. Eighteenth Annual IEEE*, volume: 2, pp 1118-1126.

[10] J. Chiasson, L. Tolbert, K. McKenzie and Z. Du, "Eliminating harmonics in a multilevel converter using resultant theory," *Power Electronics Specialists Conf., 2002*, volume: 2, pp 503-508.

[11] D. Cox, J. Little and D. O'Shea, *Using algebraic geometry*, Springer, New York, 1998.

APPENDIX

Fact [11]: Given two polynomials

$$f(x, y) = a_0(x)y^l + a_1(x)y^{l-1} + \dots + a_l, \quad a_0(x) \neq 0, \quad l > 0$$

$$g(x, y) = b_0(x)y^n + b_1(x)y^{n-1} + \dots + b_n, \quad b_0(x) \neq 0, \quad n > 0$$

all possible solutions (x^*, y^*) of $f(x, y) = 0$ and $g(x, y) = 0$ can be obtained by finding x^* as the eigenvalues of the Sylvester matrix formed from the $a_j(x)$, $j = 1, \dots, l$, and $b_k(x)$, $k = 1, \dots, n$, and then y^* as the roots of $f(x^*, y) = 0$.

Procedure for calculating the 3-step angle solutions:

- From (12a), substitute $c_3(c_1, c_2)$ into (12b) and (12c) to obtain two polynomial equations in c_1 and c_2 .
- From the two polynomials $f(c_1, c_2)$ and $g(c_1, c_2)$, extract the coefficients of the powers of c_2 and label them appropriately as $a_0, a_1, \dots, a_l, b_0, b_1, \dots, b_n$.
- Form the Sylvester matrix [11] from these coefficients and then find its eigenvalues. These eigenvalues are the candidate solutions for c_1 in our problem, which also needs to be a real number and satisfy $0 \leq c_1 \leq 1$; so discard the inadmissible ones.
- For each remaining candidate solution for c_1 , substitute its value into $f(c_1, c_2)$ and find the candidate solutions for c_2 in our problem, which needs to be a real number and satisfy $0 \leq c_2 \leq c_1$; so discard the inadmissible ones.
- For each remaining candidate solution for c_2 , substitute its value and the corresponding candidate solution for c_1 into (12a) to find the candidate solution for c_3 , which needs to be a real number and satisfy $0 \leq c_3 \leq c_2$ to be admissible.
- The admissible triples of (c_1, c_2, c_3) are then the solution(s) to the 3-step waveform problem.